Coupling reconstruction and motion estimation for dynamic MRI through optical flow constraint

Ningning Zhao, Daniel O'Connor, Wenbo Gu, Dan Ruan, Adrian Basarab, Ke Sheng

Coupling reconstruction and motion estimation for dynamic MRI through optical flow constraint

Ningning Zhao[a], Daniel O'Connor[a], Wenbo Gu[a], Dan Ruan[a], Adrian Basarab[b], and Ke Sheng[a]

[a]Department of Radiation Oncology, University of California Los Angeles, CA, USA
[b]Institut de Recherche en Informatique de Toulouse, University of Toulouse, France

ABSTRACT

This paper addresses the problem of dynamic magnetic resonance image (DMRI) reconstruction and motion estimation jointly. Because of the inherent anatomical movements in DMRI acquisition, reconstruction of DMRI using motion estimation/compensation (ME/MC) has been explored under the compressed sensing (CS) scheme. In this paper, by embedding the intensity based optical flow (OF) constraint into the traditional CS scheme, we are able to couple the DMRI reconstruction and motion vector estimation. Moreover, the OF constraint is employed in a specific coarse resolution scale in order to reduce the computational complexity. The resulting optimization problem is then solved using a primal-dual algorithm due to its efficiency when dealing with non-differentiable problems. Experiments on highly accelerated dynamic cardiac MRI with multiple receiver coils validate the performance of the proposed algorithm.

Keywords: D ynamic MRI, compressed sensing, parallel imaging, optical flow, primal-dual algorithm, line-search.

1. INTRODUCTION

Dynamic magnetic resonance imaging (DMRI) reconstruction aims at obtaining spatial-temporal MRI sequences from the measurements acquired in the k-t space. Due to the slow MRI acquisition, the trade-off between spatial and temporal resolution in DMRI reconstruction is challenging. The existing methods to deal with this issue include fast low-angle shot imaging,[1] parallel imaging[2] and compressed sensing (CS).[3,4] In the CS based framework, prior information (regularization) is helpful to regularize the ill-posed problem. The widely used regularizations in DMRI reconstruction include sparsity in transformed domains,[5] total variation (TV) penalties,[6] low-rank property[7] or a combination of several priors.[8–10] In the parallel imaging, a reduced amount of data is acquired with an array of receiver coils. The corresponding coil sensitivity maps can be estimated in advance. Therefore, the parallel imaging techniques can be readily incorporated in the CS framework, see e.g.[11]

Moreover, owing to the presence of anatomical motion in DMRI acquisition, combining the motion estimation with the DMRI reconstruction has been widely explored in the literature, see e.g.[11–14] In this paper, we couple the reconstruction and motion estimation by embedding an intensity based optical (OF) constraint into the CS framework. In order to reduce the computational cost, the OF constraint is exploited at a coarse resolution scale. Moreover, an affine model is employed to model local tissue deformations.[15] The resulting formulated problem is addressed using the primal-dual algorithm with linesearch,[16] which is efficient to handle non-differentiable optimization problems. Experiments on the reconstruction of dynamic cardiac MRI are conducted to demonstrate the efficiency of the proposed framework.

The remainder of this paper is organized as follows. The problem formulation is described in section 2. Section 3 details the proposed algorithm and relevant derivations. Section 4 gives the experimental results. Conclusions and perspectives are reported in Section 5.

Further author information:
Author E-mail: Ningning Zhao, Daniel O'Connor, Wenbo Gu, Dan Ruan and Ke Sheng: {NZhao, DOconnor,WGu, DRuan, KSheng}@mednet.ucla.edu, Adrian Basarab: adrian.basarab@irit.fr

2. PROBLEM FORMULATION

2.1 Measurement model

Denoting $\mathbf{f}$ whose rows correspond to the voxels and columns represent the temporal frames as the DMRI sequences, the DMRI can be modelled using the following matrix form equation

$$\mathbf{b} = \mathcal{A}\mathbf{f} + \mathbf{n}, \tag{1}$$

where $\mathbf{b}$ is the measurement, $\mathbf{f}$ is the dynamic image sequences to be estimated, $\mathbf{n}$ is the measurement noise and the measurement operator $\mathcal{A} = \mathbf{SF}$, where $\mathbf{F}$ is the partial Fourier transform at specific sampling locations and $\mathbf{S}$ is the coil sensitivity map, which can estimated in advance.

2.2 Prerequisite

Optical flow constraint

Denoting $\mathbf{f}(\mathbf{x}, t)$ as the tth frame MRI sequences at the location $\mathbf{x} = (x, y)$ (only 2D cases are considered in this work), the brightness constancy constraint in DMRI is expressed by

$$\mathbf{f}(\mathbf{x}, t) = \mathbf{f}(\mathbf{x} - \mathbf{d}(\mathbf{x}, t), t_0), \tag{2}$$

where $\mathbf{d}(\mathbf{x}, t) = [\mathbf{u}(\mathbf{x}, t), \mathbf{v}(\mathbf{x}, t)]^T$ is the displacement field. Under the small displacement assumption, we have

$$\mathbf{f}(\mathbf{x} - \mathbf{d}(\mathbf{x}, t), t_0) \approx \mathbf{f}(\mathbf{x}, t_0) - \partial_x \mathbf{f}(\mathbf{x}, t_0)\mathbf{u}(\mathbf{x}, t) - \partial_y \mathbf{f}(\mathbf{x}, t_0)\mathbf{v}(\mathbf{x}, t). \tag{3}$$

Thus, the OF constraint equation is given by

$$\mathbf{f}(\mathbf{x}, t) - \mathbf{f}(\mathbf{x}, t_0) + \partial_x \mathbf{f}(\mathbf{x}, t_0)\mathbf{u}(\mathbf{x}, t) + \partial_y \mathbf{f}(\mathbf{x}, t_0)\mathbf{v}(\mathbf{x}, t) = 0. \tag{4}$$

In addition, since the motion patterns in DMRI can be very complicated, e.g., rotation, expansion and shear, the affine model for the motion vectors $[\mathbf{u}, \mathbf{v}]^T$ has been introduced[15,17] as following

$$\mathbf{u}(\mathbf{x}, t) = \mathbf{u}_0(\mathbf{x}, t) + \mathbf{u}_1(\mathbf{x}, t)x + \mathbf{u}_2(\mathbf{x}, t)y \tag{5}$$

$$\mathbf{v}(\mathbf{x}, t) = \mathbf{v}_0(\mathbf{x}, t) + \mathbf{v}_1(\mathbf{x}, t)x + \mathbf{v}_2(\mathbf{x}, t)y, \tag{6}$$

where $\mathbf{u}_0$, $\mathbf{u}_1$, $\mathbf{u}_2$ and $\mathbf{v}_0$, $\mathbf{v}_1$, $\mathbf{v}_2$ are the affine parameters defining the deformation field of pixels at position (x, y) in frame t w.r.t. the reference frame $\mathbf{f}(\mathbf{x}, t_0)$.

Moreover, the weighted OF equation expressed in (7) has been exploited to estimate the motion vectors in different resolution scale, see e.g.,.[15,17]

$$\int_{\mathbf{x}} \mathbf{w}(\mathbf{x} - \mathbf{x}_0) \left[\mathbf{f}(\mathbf{x}, t) - \mathbf{f}(\mathbf{x}, t_0) + \partial_x \mathbf{f}(\mathbf{x}, t_0)\mathbf{u}(\mathbf{x}, t) + \partial_y \mathbf{f}(\mathbf{x}, t_0)\mathbf{v}(\mathbf{x}, t)\right] d\mathbf{x}, \tag{7}$$

where $\mathbf{w}$ is a window function centered at $\mathbf{x}_0$. In this work, B-spline based function has been used to build the window function. Varying the B-spline degree changes the size of $\mathbf{w}$. Dilating and shifting the window function leads to an OF equation at different spatial scale. Specifically, at a coarse scale j, the window function is given by

$$\mathbf{w}^{(j)}(\mathbf{x} - \mathbf{x}_0) = \mathbf{w}\left(\frac{\mathbf{x} - 2^j \mathbf{x}_0}{2^j}\right). \tag{8}$$

Proximal operator

The proximal operator of function g (lower semicontinuous) is defined as

$$\mathrm{prox}_{sg}(p) = \arg\min_x g(x) + \frac{1}{2s}\|x - p\|^2. \tag{9}$$

Note that the proximal operator calculation always has a unique solution.

Primal dual algorithm

Given an optimization problem as below

$$\min_{\mathbf{y}} g(\mathbf{C}\mathbf{y}) + h(\mathbf{y}), \tag{10}$$

where h and g are proper, convex and lower semicontinuous functions, $\mathbf{C}$ is a continuous linear operator. The primal dual algorithm (PDA) to deal with the problem (10) is given by

$$\begin{array}{l} \text{For } k = 1, \dots \\ \left\lfloor \begin{array}{l} \mathbf{y}^k = \mathrm{prox}_{\sigma h}\left(\mathbf{y}^{k-1} - \sigma \mathbf{C}^* \mathbf{z}^{k-1}\right) \\ \mathbf{z}^k = \mathrm{prox}_{s g_l^*}(\mathbf{z}^{k-1} + s\mathbf{C}(2\mathbf{y}^k - \mathbf{y}^{k-1})) \end{array} \right. \end{array} \tag{11}$$

where $\mathbf{C}^*$ represents the adjoint of matrix $\mathbf{C}$ and g^* is the conjugate of function g. Note that the stepsize parameters in PDA need to satisfy the relationship $s\sigma\|\mathbf{C}\| \leq 1$ to ensure the convergence. More details about the PDA can turn to the literatures, see e.g.[18]

2.3 Problem formulation

We denote the DMRI acquired at instance t_0, i.e., $\mathbf{f}(\mathbf{x}, t_0)$ as the reference frame. Note that a reference frame can be obtained from a fully-sampled data. Moreover, by replicating the $\mathbf{f}(\mathbf{x}, t_0)$ and stack them into a cube of the same size as the image sequences to be estimated, we obtain a reference cube, denoted as $\bar{\mathbf{f}}_0$.

The problem of jointly reconstructing the DMRI and estimating the motion vectors can then be formulated as blow

$$\min_{\mathbf{f},\mathbf{d}} \|\mathcal{A}\mathbf{f} - \mathbf{b}\|_2^2 + \eta_1\|\mathbf{f}\|_* + \eta_2\|\nabla\mathbf{f}\|_1 + \tau\|\mathcal{M}_{\mathbf{w}^{(j)}}(\mathbf{f}, \bar{\mathbf{f}}_0, \mathbf{d})\|_1 + \psi(\mathbf{d}), \tag{12}$$

where $\|\cdot\|_*$ and $\|\cdot\|_1$ represent the nuclear norm and ℓ_1 norm of variables, $\eta_1\|\mathbf{f}\|_* + \eta_2\|\nabla\mathbf{f}\|_1$ is a joint regularization term for the DMRI (low rank plus TV), $\mathcal{M}_{\mathbf{w}^{(j)}}(\mathbf{f}, \bar{\mathbf{f}}_0, \mathbf{d})$ is the weighted OF equation at scale j given by

$$\begin{aligned} &\mathcal{M}_{\mathbf{w}^{(j)}}(\mathbf{f}, \bar{\mathbf{f}}_0, \mathbf{d}) = \langle \mathbf{f} - \bar{\mathbf{f}}_0 \rangle_{\mathbf{w}^{(j)}} + \langle \partial_x \bar{\mathbf{f}}_0 \rangle_{\mathbf{w}^{(j)}} \mathbf{u} + \langle \partial_y \bar{\mathbf{f}}_0 \rangle_{\mathbf{w}^{(j)}} \mathbf{v} \\ =&\langle \mathbf{f} - \bar{\mathbf{f}}_0 \rangle_{\mathbf{w}^{(j)}} + \langle \partial_x \bar{\mathbf{f}}_0 \rangle_{\mathbf{w}^{(j)}} \mathbf{u}_0 + \langle x\partial_x \bar{\mathbf{f}}_0 \rangle_{\mathbf{w}^{(j)}} \mathbf{u}_1 + \langle y\partial_x \bar{\mathbf{f}}_0 \rangle_{\mathbf{w}^{(j)}} \mathbf{u}_2 + \langle \partial_y \bar{\mathbf{f}}_0 \rangle_{\mathbf{w}^{(j)}} \mathbf{v}_0 + \langle x\partial_y \bar{\mathbf{f}}_0 \rangle_{\mathbf{w}^{(j)}} \mathbf{v}_1 + \langle y\partial_y \bar{\mathbf{f}}_0 \rangle_{\mathbf{w}^{(j)}} \mathbf{v}_2 \end{aligned} \tag{13}$$

where $\langle \mathbf{r} \rangle_{\mathbf{w}^{(j)}}$ is the weighted average of variable $\mathbf{r} \in \{\mathbf{f} - \bar{\mathbf{f}}_0, \partial_x\bar{\mathbf{f}}_0, x\partial_x\bar{\mathbf{f}}_0, y\partial_x\bar{\mathbf{f}}_0, \partial_y\bar{\mathbf{f}}_0, x\partial_y\bar{\mathbf{f}}_0, y\partial_y\bar{\mathbf{f}}_0\}$ at scale j, which is written as

$$\langle \mathbf{r} \rangle_{\mathbf{w}^{(j)}} = \int_{\mathbf{x}} \mathbf{w}^{(j)}(\mathbf{x} - \mathbf{x}_0)\mathbf{r}(\mathbf{x})d\mathbf{x}. \tag{14}$$

$\psi(\mathbf{d})$ is the regularization for the motion vector. We consider the isotropic TV prior to smooth the displacement field. Thus, we have

$$\psi(\mathbf{d}) = \gamma\sum_{i=0}^{2}\|\nabla\mathbf{u}_i\|_1 + \gamma\sum_{i=0}^{2}\|\nabla\mathbf{v}_i\|_1. \tag{15}$$

3. METHODOLOGY

The formulated problem is addressed using the primal dual algorithm with linesearch (PDAL),[16] known to be efficient in handling non-differentiable convex optimization problems. In order to use PDAL to address (12), we rewrite it as blow

$$\min_{\mathbf{y}} g(\mathbf{C}\mathbf{y}) = \sum_{l=1}^{10} g_l(\mathbf{C}_l\mathbf{y}) \triangleq \sum_{l=1}^{10} g_l(\mathbf{\Omega}_l) \tag{16}$$

where $\mathbf{y} = [\mathbf{f}, \mathbf{u}_0, \mathbf{u}_1, \mathbf{u}_2, \mathbf{v}_0, \mathbf{v}_1, \mathbf{v}_2]^T$ is the variable to be estimated, $\mathbf{\Omega}_l = \mathbf{C}_l\mathbf{y}$, the matrix $\mathbf{C}$ is expressed by

$$
\mathbf{C}=\begin{bmatrix}\mathbf{C}_1\\ \mathbf{C}_2\\ \mathbf{C}_3\\ \mathbf{C}_4\\ \mathbf{C}_5\\ \mathbf{C}_6\\ \mathbf{C}_7\\ \mathbf{C}_8\\ \mathbf{C}_9\\ \mathbf{C}_{10}\end{bmatrix}=\begin{bmatrix}\mathcal{A} & 0 & 0 & 0 & 0 & 0 & 0\\ \langle\cdot\rangle_{\mathbf{w}^{(j)}} & \langle\partial_x\bar{\mathbf{f}}_0\rangle_{\mathbf{w}^{(j)}} & \langle x\partial_x\bar{\mathbf{f}}_0\rangle_{\mathbf{w}^{(j)}} & \langle y\partial_x\bar{\mathbf{f}}_0\rangle_{\mathbf{w}^{(j)}} & \langle\partial_y\bar{\mathbf{f}}_0\rangle_{\mathbf{w}^{(j)}} & \langle x\partial_y\bar{\mathbf{f}}_0\rangle_{\mathbf{w}^{(j)}} & \langle y\partial_y\bar{\mathbf{f}}_0\rangle_{\mathbf{w}^{(j)}}\\ \mathbf{I} & 0 & 0 & 0 & 0 & 0 & 0\\ \mathcal{T} & 0 & 0 & 0 & 0 & 0 & 0\\ 0 & \nabla & 0 & 0 & 0 & 0 & 0\\ 0 & 0 & \nabla & 0 & 0 & 0 & 0\\ 0 & 0 & 0 & \nabla & 0 & 0 & 0\\ 0 & 0 & 0 & 0 & \nabla & 0 & 0\\ 0 & 0 & 0 & 0 & 0 & \nabla & 0\\ 0 & 0 & 0 & 0 & 0 & 0 & \nabla\end{bmatrix} \tag{17}
$$

The ten functions are expressed as

$$
\begin{cases} g_1(\mathbf{\Omega}_1)=\frac{1}{2}\|\mathbf{\Omega}_1-\mathbf{b}\|_2^2,\\ g_2(\mathbf{\Omega}_2)=\tau\|\mathbf{\Omega}_2-\langle\bar{\mathbf{f}}_0\rangle_{\mathbf{w}^{(j)}}\|_1,\\ g_3(\mathbf{\Omega}_3)=\eta\|\mathbf{\Omega}_3\|_*,\\ g_4(\mathbf{\Omega}_4)=\eta\|\mathbf{\Omega}_3\|_1,\\ g_l(\mathbf{\Omega}_d)=\gamma\|\mathbf{\Omega}_d\|_1,\ \text{for } d=5,\dots,10,\end{cases} \tag{18}
$$

By introducing the dual variables $\mathbf{z}=[\mathbf{z}_1,\dots,\mathbf{z}_{10}]^T$, the PDA to solve problem (16) is given by

$$
\begin{array}{l}\text{For } k=1,\dots\\ \left\lfloor\begin{array}{l}\mathbf{y}^k=\mathbf{y}^{k-1}-\sigma\left(\sum_{l=1}^{10}\mathbf{C}_l^*\mathbf{z}_l^{k-1}\right)\\ \mathbf{z}_l^k=\mathrm{prox}_{sg_l^*}(\mathbf{z}_l^{k-1}+s\mathbf{C}_l(2\mathbf{y}^k-\mathbf{y}^{k-1}))\end{array}\right.\end{array} \tag{19}
$$

In order to accelerate (19), we use the PDA with linesearch to address (16), which is summarized as below

Algorithm 1 Joint MRI reconstruction and motion estimation using PDAL (J-PDAL)

Require: $\mathbf{y}^0=[\mathbf{f}^0,\mathbf{u}_0^0,\mathbf{u}_1^0,\mathbf{u}_2^0,\mathbf{v}_0^0,\mathbf{v}_1^0,\mathbf{v}_2^0]$, $\mathbf{z}_l^0$, $l\in\{1\cdots 10\}$, $\sigma^0>0$, $\alpha>0$, $\epsilon\in(0,1)$, $\rho\in(0,1)$

Set $\theta^0=1$

for k = 1 … **do** ▷ Update $\mathbf{y}=[\mathbf{f},\mathbf{u}_0,\mathbf{u}_1,\mathbf{u}_2,\mathbf{v}_0,\mathbf{v}_1,\mathbf{v}_2]$

  $\mathbf{y}^k=\mathbf{y}^{k-1}-\sigma^{k-1}\left(\sum_{l=1}^{10}\mathbf{C}_l^T\mathbf{z}_l^{k-1}\right)$

  Choose any $\sigma^k\in[\sigma^{k-1},\sigma^{k-1}\sqrt{1+\theta^{k-1}}]$

  Linesearch ▷ Start linesearch

  $\bar{\mathbf{y}}^k=\mathbf{y}^k+\theta^k(\mathbf{y}^k-\mathbf{y}^{k-1})$

  for l=1, …, 10 **do**

    $\mathbf{z}_l^k=\mathrm{prox}_{\alpha\sigma^k g_l^*}(\mathbf{z}_l^{k-1}+s\mathbf{C}_l\bar{\mathbf{y}}^k)$ ▷ Update $\mathbf{z}_l$ by calculating the proximal operator of $g_l^*(\cdot)$

  if $\sqrt{\alpha}\sigma^k\|\mathbf{C}^T\mathbf{z}^k-\mathbf{C}^T\mathbf{z}^{k-1}\|\le\epsilon\|\mathbf{z}^k-\mathbf{z}^{k-1}\|$ **then**

    break the linesearch ▷ Break linesearch

  else

    $\sigma^k=\sigma^k\rho$ and go to ***linesearch***

  Until stopping criterion is satisfied. ▷ Stopping criterion

Note that the calculations of the proximal operators of g_l^* are given as following

$$
\begin{cases}\mathrm{prox}_{sg_1^*}(\tilde{\mathbf{z}}_1)=\frac{\tilde{\mathbf{z}}_1-s\mathbf{b}}{1+s},\\ \mathrm{prox}_{sg_2^*}(\tilde{\mathbf{z}}_2)=\mathrm{Proj}_{\tau P}\left(\tilde{\mathbf{z}}_2-s\langle\bar{\mathbf{I}}_0\rangle_{\mathbf{w}^{(j)}}\right),\\ \mathrm{prox}_{sg_d^*}(\tilde{\mathbf{z}}_d)=\mathrm{Proj}_{\gamma P}(\tilde{\mathbf{z}}_l),\ \text{for } l=4,\dots,9,\\ \mathrm{prox}_{sg_{10}^*}(\tilde{\mathbf{z}}_{10})=\mathrm{Proj}_{\lambda P}(\tilde{\mathbf{z}}_{10}),\end{cases} \tag{20}
$$

where $\mathrm{Proj}_{\tau P}$ is a projector onto the convex set (Euclidean ℓ^2-ball) $\tau P = \{\|p\|_\infty \leq \tau\}$, where $\|p\|_\infty = \max_{i,j} |p_{i,j}|$. In practice, this projector can be computed using the straightforward formula

$$\mathrm{Proj}_{\tau P}(p) = \frac{p}{\max\{\tau, |p|\}}. \tag{21}$$

4. EXPERIMENTAL RESULTS

In this section, We conducted experiments on *in vivo* cardiac perfusion (without parallel imaging) and cardiac cine (with parallel imaging) data. The proposed algorithm was also compared with the L+S algorithm.[13]

The myocardial perfusion MRI data* was acquired using a saturation recovery FLASH sequence at the University of Utah, courtesy of Dr. Edward DiBella.[8] The radial sampling trajectory was employed in this simulation with a decimation factor 6. The data is of size $90 \times 190 \times 70$. Fig. 1 displays the fully sampled data and the reconstructed image sequences for the cardiac perfusion data using the proposed J-PDAL and the algorithm L+S†. The RMSEs of the two algorithms for each frame are also shown in Fig. 1. The proposed algorithm outperforms the L+S algorithm in terms of the RMSEs.

The cardiac cine data was acquired in a healthy adult volunteer with a modified TurboFLASH pulse sequence on a whole-body 3T scanner (Tim Trio, Siemens Healthcare, Erlangen, Germany) using a 12-element matrix coil array.[13] This data is of size $256 \times 256 \times 24$. The Cartesian downsampling trajectory was employed with a decimation factor 6. Fig. 2 shows the reconstructed images for the cardiac cine data using the J-PDAL and L+S. More clearly boundaries can be observed in the reconstructed image sequences using the proposed J-PDAL. Due to the absence of groundtruth of the cardiac cine data, the resolution gain (RG)[19] is employed for the quantitative evaluation of the reconstruction performance. RG is the ratio of the normalized autocorrelation (higher than -3 dB) of the initial MRI sequences (i.e., $\mathcal{A}^T\mathbf{b}$) to the normalized autocorrelation (higher than -3 dB) of the restored MRI sequences. Fig. 3 displays the RGs using the two algorithms for each frame of the cardiac cine data. Note that the RGs are calculated for the region of interest (ROI), shown in the blue box in Fig. 2.

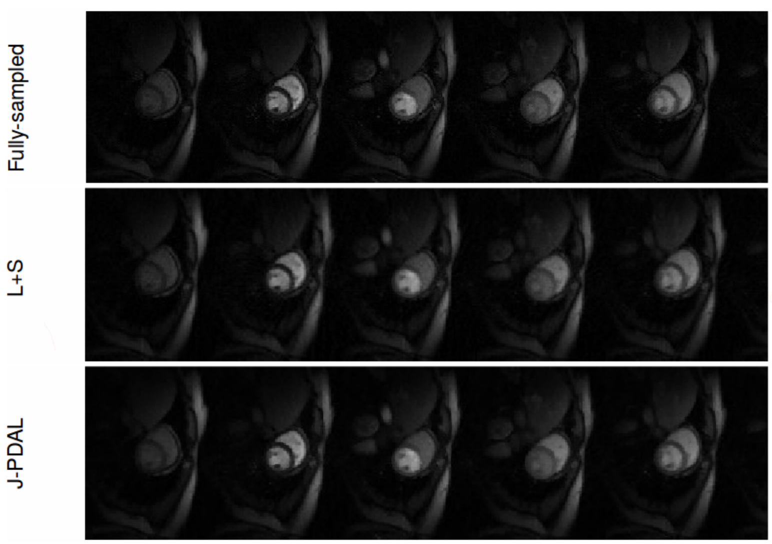

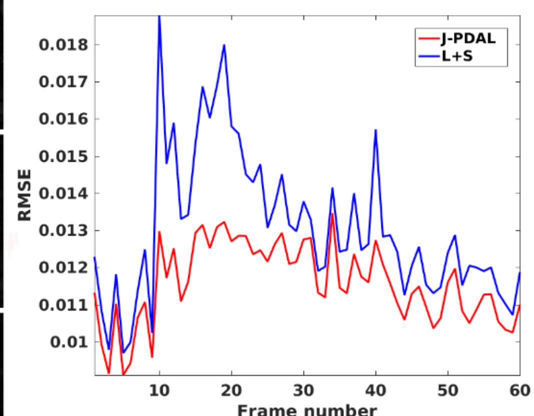

Figure 1. Left: fully sampled (top) and reconstructed cardiac perfusion data using L+S (middle) and J-PDAL (bottom); Right: RMSEs calculated for different temporal frames using L+S (blue) and J-PDAL (red).

*The dataset implemented in this paper can be downloaded `https://research.engineering.uiowa.edu/cbig/content/matlab-codes-blind-compressed-sensing-bcs-dynamic-mri`

†The matlab implementation of the L+S algorithm can be found `http://cai2r.net/research/ls-reconstruction`

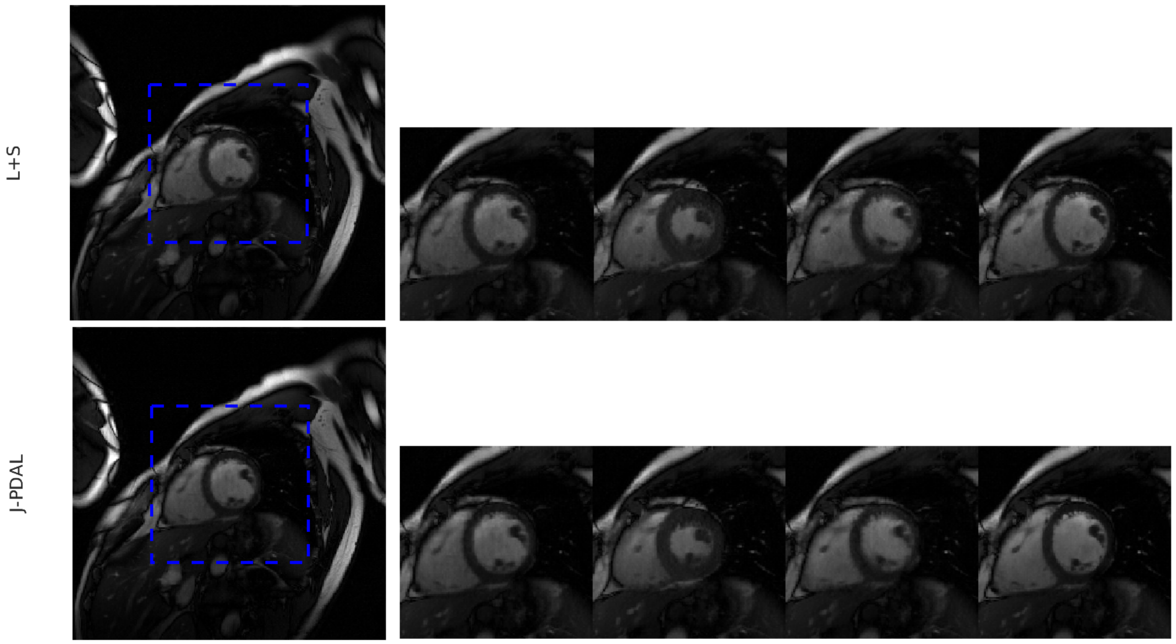

Figure 2. Reconstruction of cardiac cine data using L+S (top) and the proposed J+PDAL (bottom).

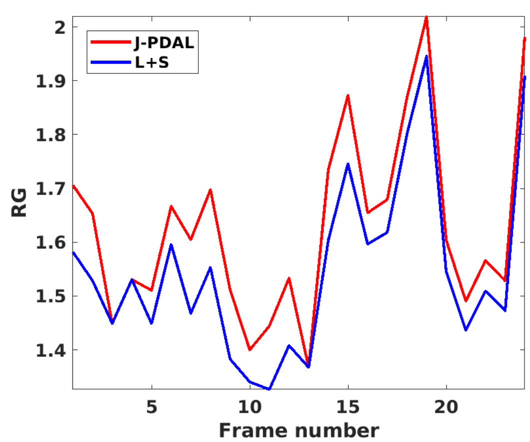

Figure 3. Resolution gain (RG) of the reconstruction of cardiac cine image sequences using L+S (blue) and the proposed J+PDAL (red).

5. CONCLUSIONS

The proposed algorithm is able to integrate the image reconstruction and motion estimation. The joint low rank plus total variation regularization is an appropriate prior for the dynamic cardiac dataset explored in this paper. From the experimental results, the DMRI reconstruction quality on the *in vivo* cardiac data using the proposed J-PDAL outperforms the performance of the L+S algorithm. Future works include the estimation of the reference image and multi-resolution strategies for motion estimation.

Acknowledgements

This work has been supported by NIH grant R01CA188300.

REFERENCES

[1] Haase, A., Frahm, J., Matthaei, D., Hnicke, W., and Merboldt, K.-D., "FLASH imaging: Rapid NMR imaging using low flip-angle pulses," *J. Magn. Reson.* **213**(2), 533 – 541 (2011).

[2] Tsao, J. and Kozerke, S., "MRI temporal acceleration techniques," *J. Magn. Reson. Imaging* **36**(3), 543–560 (2012).

[3] Lustig, M., Donoho, D., and Pauly, J. M., "Sparse MRI: The application of compressed sensing for rapid MR imaging," *Magn. Reson. Med.* **58**(6), 1182–1195 (2007).

[4] Lustig, Michael and Donoho, David L and Santos, Juan M and Pauly, J. M., "Compressed sensing MRI," *IEEE Sig. Process. Mag.* **25**(2), 72–82 (2008).

[5] Jung, H., Sung, K., Nayak, K. S., Kim, E. Y., and Ye, J. C., "K-t FOCUSS: A general compressed sensing framework for high resolution dynamic MRI," *Magn. Reson. Med.* **61**(1), 103–116 (2009).

[6] Knoll, F., Clason, C., Bredies, K., Uecker, M., and Stollberger, R., "Parallel imaging with nonlinear reconstruction using variational penalties," *Magn. Reson. Med.* **67**(1), 34–41 (2012).

[7] Miao, X., Lingala, S. G., Guo, Y., Jao, T., Usman, M., Prieto, C., and Nayak, K. S., "Accelerated cardiac cine MRI using locally low rank and finite difference constraints," *Magn. Reson. Imaging* **34**(6), 707–714 (2016).

[8] Lingala, S. G., Hu, Y., Dibella, E., and Jacob, M., "Accelerated dynamic MRI exploiting sparsity and low-rank structure: K-t SLR," *IEEE Trans. Med. Imag.* **30**(5), 1042–1054 (2011).

[9] Majumdar, A., "Real-time Dynamic MRI Reconstruction using Stacked Denoising Autoencoder," (2015).

[10] Tremoulheac, B., Dikaios, N., Atkinson, D., and Arridge, S. R., "Dynamic MR image reconstruction-separation from undersampled (k,t)-Space via low-rank plus sparse prior," *IEEE Trans. Med. Imag.* **33**(8), 1689–1701 (2014).

[11] Asif, M. S., Hamilton, L., Brummer, M., and Romberg, J., "Motion-adaptive spatio-temporal regularization for accelerated dynamic MRI," *Magn. Reson. Med.* **70**, 800–812 (2013).

[12] Usman, M., Atkinson, D., Odille, F., Kolbitsch, C., Vaillant, G., Schaeffter, T., Batchelor, P. G., and Prieto, C., "Motion corrected compressed sensing for free-breathing dynamic cardiac MRI," *Magn. Reson. Med.* **70**, 504–516 (2013).

[13] Otazo, R., Candès, E., and Sodickson, D. K., "Low-rank plus sparse matrix decomposition for accelerated dynamic MRI with separation of background and dynamic components," *Magn. Reson. Med.* **73**(3), 1125–1136 (2015).

[14] Lingala, S. G., Member, S., Dibella, E., Jacob, M., and Member, S., "(DC-CS): A Novel Framework for Accelerated Dynamic MRI," *IEEE Trans. Med. Imag.* **34**(1), 72–85 (2015).

[15] Sühling, M., Arigovindan, M., Jansen, C., Hunziker, P., and Unser, M., "Myocardial motion analysis from B-mode echocardiograms," *IEEE Trans. Image Process.* **14**(4), 525–536 (2005).

[16] Malitsky, Y. and Pock, T., "A first-order primal-dual algorithm with linesearch," 1–24 (2016).

[17] Alessandrini, M., Basarab, A., Liebgott, H., and Bernard, O., "Myocardial Motion Estimation from Medical Images Using the Monogenic Signal," *IEEE Trans. Image Process.* **22**(3), 1084–1095 (2013).

[18] Chambolle, A. and Pock, T., "A first-order primal-dual algorithm for convex problems with applications to imaging," *J. Math. Imag. Vision* **40**(1), 120–145 (2011).

[19] Zhao, N., Basarab, A., Kouamé, D., and Tourneret, J.-Y., "Joint segmentation and deconvolution of ultrasound images using a hierarchical Bayesian model based on generalized Gaussian priors," *IEEE Trans. Image Process.* **25**(8), 3736 – 3750 (2016).